

# Measurement of the Temperature Dependence of the Casimir-Polder Force

J. M. Obrecht<sup>1,\*</sup>, R. J. Wild<sup>1</sup>, M. Antezza<sup>2</sup>, L. P. Pitaevskii<sup>2,3</sup>, S. Stringari<sup>2</sup>, E. A. Cornell<sup>1,†</sup>

<sup>1</sup>*JILA, National Institute of Standards and Technology and University of Colorado,  
and Department of Physics, University of Colorado, Boulder, Colorado 80309-0440, USA*

<sup>2</sup>*Dipartimento di Fisica, Università di Trento and CNR-INFM BEC Center, Via Sommarive 14, I-38050 Povo, Trento, Italy*

<sup>3</sup>*Kapitza Institute for Physical Problems, ul. Kosygina 2, 119334 Moscow, Russia*

(Dated: May 25, 2019)

We report on the first measurement of a temperature dependence of the Casimir-Polder force. This measurement was obtained by positioning a nearly pure  $^{87}\text{Rb}$  Bose-Einstein condensate a few microns from a dielectric substrate and exciting its dipole oscillation. Changes in the collective oscillation frequency of the magnetically trapped atoms result from spatial variations in the surface-atom force. In our experiment, the dielectric substrate is heated up to 605 K, while the surrounding environment is kept near room temperature (310 K). The effect of the Casimir-Polder force is measured to be nearly three times larger for a 605 K substrate than for a room-temperature substrate, showing a clear temperature dependence in agreement with theory.

PACS numbers: 03.75.Kk, 34.50.Dy, 31.30.Jv, 42.50.Vk, 42.50.Nn

The Casimir force and its molecular cousin, the van der Waals force, are not only fascinating scientifically but also important technologically, for example in atomic force microscopy and MEMS. Like the tension in a rubber band, the Casimir force is a conservative force arising from microscopic fluctuations. The Casimir force is also the dominant background effect confounding attempts [1, 2, 3, 4] to set improved limits on exotic forces at the  $10^{-8}$  m to  $10^{-5}$  m length scale; progress towards a deeper understanding is valuable in that context. Typically one uses “Casimir” [5] to refer to the force between two bulk objects, such as metallic spheres or dielectric plates, and “Casimir-Polder” (C-P) [6] to describe the force between a bulk object and a gas-phase atom. The underlying physics [7] is largely the same, however, and, particularly in the limit of separations exceeding one micron, it can be more convenient to study the latter system due to ease in rejecting systematic errors such as electrostatic patch potentials [8, 9].

The Casimir force arises from fluctuations of the electromagnetic field and is usually thought of as being purely quantum-mechanical. However, at nonzero temperatures, the fluctuations also have a thermal contribution, which was investigated by Lifshitz [10]. Precise theoretical modeling of Casimir forces takes into account effects such as surface roughness, finite conductivity, substrate geometry, and nonzero temperature, but the latter term has never been unambiguously observed experimentally (see [11] and references therein). In earlier Casimir [4, 12, 13, 14, 15, 16] and Casimir-Polder [9, 17, 18, 19, 20, 21, 22, 23] experiments, thermal effects were predicted to be on the order of experimental uncertainties or less because (a) the temperature of the apparatus could not be varied over a large range and (b) the experiments worked over small separations compared to the wavelength of thermal radiation, where thermal corrections are small.

In this Letter, we report the first measurement of a

temperature dependence of the Casimir-Polder force, indeed the first conclusive temperature dependence of any Casimir-like system. A key feature of this work is that the apparatus temperature is spatially nonuniform. This allows for an experimental confirmation of an appealing theoretical insight: The thermal electromagnetic-field fluctuations that drive the C-P force can be separated into two categories — those that undergo internal and those that undergo external reflection at the surface. These two categories of fluctuations contribute to the total force with opposite sign; in thermal equilibrium, they very nearly cancel, masking the underlying scale of thermal effects. Working outside thermal equilibrium, we observe thermal contributions to the C-P force that are three times as large as the zero-temperature force.

To review the main regimes in surface-atom forces: For a surface-atom separation  $x$  much less than the wavelength of the dominant resonances in the atom and substrate, the potential  $U$  scales as  $1/x^3$  (van der Waals-London regime). At longer distances, retardation effects cause a crossover to  $U \sim 1/x^4$  (Casimir-Polder). At still longer distances when  $x$  is comparable to the blackbody peak at temperature  $T$ , temperature effects become important, and in thermal equilibrium ( $T = T_S = T_E$ , as defined below), there is a second crossover, back to  $U \sim T/x^3$  (Lifshitz).

Recent theoretical work [24] has shown that thermal corrections to the Casimir-Polder force are separable into those arising from thermal fluctuations within the substrate at temperature  $T_S$  [25] and those arising from radiation impinging from presumed distant walls at an environmental temperature  $T_E$ . At  $T_S \neq 0$ , electromagnetic fluctuations from within the surface have an evanescent component that extends into the vacuum with maximum intensity at the surface, giving rise to an attractive AC Stark potential (Fig. 1). Impinging external radiation at  $T_E$  reflects from the surface, giving rise to a standing wave whose intensity is at a minimum near the sur-

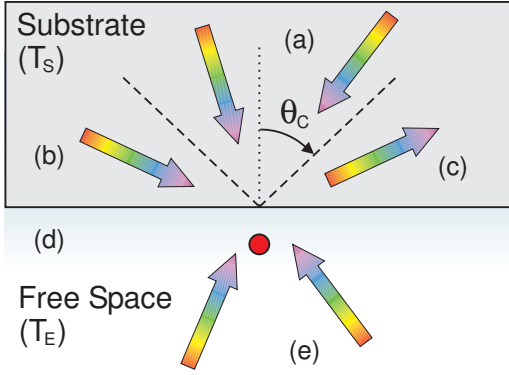


FIG. 1: (Color online) Cartoon drawing of thermal fluctuations near the surface of a dielectric substrate (shaded region). (a) Internal radiation striking the surface at angles less than the critical angle  $\theta_c$  does not contribute to the Casimir-Polder force. However, internal radiation impinging at larger angles (b) undergoes total internal reflection (c) and contributes to an overall AC Stark shift by creating evanescent waves in free space (d). Surrounding the atom (red circle) is radiation from the environment (e) which contributes to the C-P force by creating standing waves at the surface. The force does not arise from radiation pressure but rather from gradients in intensity. The surface-atom force becomes more attractive for  $T_S > T_E$  and more repulsive for  $T_S < T_E$ .

face. The Stark shift then pulls the atom *away* from the surface, contributing a repulsive term to the potential [26]. Antezza *et al.* [24] recently predicted that the nonequilibrium contribution to the C-P potential asymptotically scales as  $U_{NEQ} \sim (T_S^2 - T_E^2)/x^2$ . This novel scaling dependence dominates at long range. One can thus temperature-tune the magnitude of this long-range force and, in principle, even change the sign of the overall force.

We observe the temperature dependence of the Casimir-Polder force between a rubidium atom and a dielectric substrate by measuring the collective oscillation frequency of the mechanical dipole mode of a Bose-Einstein condensate (BEC) near enough to a dielectric substrate for the C-P force to measurably distort the trapping potential. This distortion of the trap results in changes to the oscillation frequency proportional to the gradient of the force:

$$\gamma_x \equiv \frac{\omega_o - \omega_x}{\omega_o} \simeq \frac{1}{2m\omega_o^2} \langle \partial_x F_{CP} \rangle, \quad (1)$$

where  $m$  is the mass of the  $^{87}\text{Rb}$  atom, and  $\gamma_x$  is defined as the fractional frequency difference between the unperturbed trap frequency  $\omega_o$  and  $\omega_x$ , the trap frequency perturbed by the C-P force  $F_{CP}$ .

The use of a BEC in this work is not conceptually central. The force between the substrate and the condensate is the simple sum of the force on the individual atoms of the condensate. For our purpose, the condensate repre-

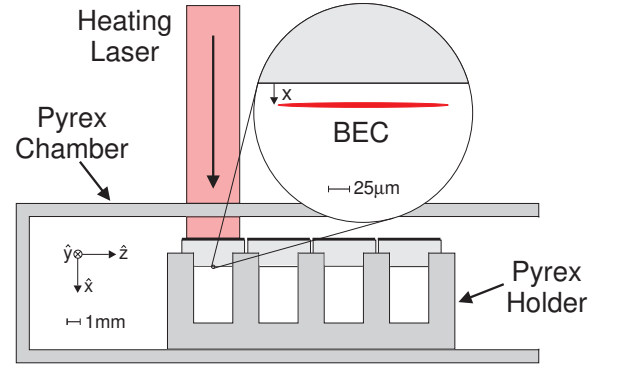


FIG. 2: (Color online) Side view of the apparatus. Shown is a scale drawing of the fused silica substrate (left-most of the four substrates) with a top layer of graphite. The graphite absorbs the light from the laser, heating the substrate. The pyrex holder is isolated enough from the substrate to allow a hot substrate – cool environment scenario. The enlargement in the inset shows the BEC at a distance  $x$  from the surface.

sents a spatially compact collection of a relatively large number of atoms whose well-characterized Thomas-Fermi density profile facilitates the spatial averaging and the inclusion of nonlinear effects in the oscillations, necessary for the quantitative comparison between theory and experiment [9, 27].

A detailed description of the experimental apparatus, along with surface-atom measurement and calibration techniques, appears in [8, 9, 28]. In brief, the experiment consists of  $2.5 \times 10^5$   $^{87}\text{Rb}$  atoms Bose-condensed (condensate purity  $> 0.8$ ) in the  $|F=1, m_F=-1\rangle$  ground state. The condensate is produced  $\sim 1.2$  mm below a dielectric substrate by forced rf evaporation in a Ioffe-Pritchard-style magnetic trap (trap frequencies of 229 Hz and 6.4 Hz in the radial and axial directions, respectively), resulting in respective Thomas-Fermi radii of  $2.69 \mu\text{m}$  and  $97.1 \mu\text{m}$ .

The dielectric substrate studied consists of uv-grade fused silica  $\sim 2 \times 8 \times 5 \text{ mm}^3$  in size ( $x, y, z$  directions, respectively) sitting atop a monolithic pyrex glass holder inside a pyrex glass cell which composes the vacuum chamber (Fig. 2). The top surface ( $-\hat{x}$  face) of the substrate is painted with a  $\sim 100 \mu\text{m}$  thick opaque layer of graphite and treated in a high-temperature oven prior to placement in the vacuum chamber to prevent outgassing and maintain ultrahigh vacuum standards for present work.

The fused silica substrate was heated by shining  $\sim 1$  W of laser light (860 nm) on the graphite layer. The rough texture of the pyrex holder creates near point contacts with the substrate corners, providing good thermal isolation between the holder and the substrate. This technique allows us to vary the temperature of the substrate while maintaining near room temperature vacuum chamber walls and only slightly elevated holder temperatures.

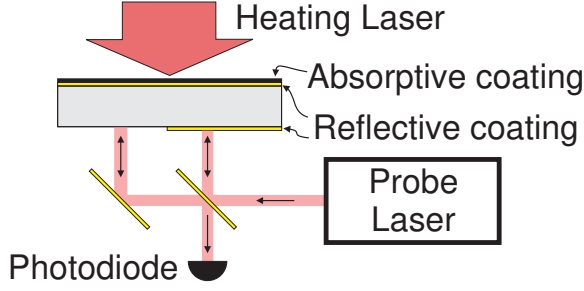


FIG. 3: (Color online) Interferometric temperature measurement apparatus (sizes not to scale). Shown is a schematic view of the Michelson interferometer used to non-perturbatively measure the substrate temperature. As the substrate heats, the glass both expands *and* changes its index of refraction, creating an interferometric signal.

The temperature of the fused-silica substrate as a function of the heating laser power was determined in an offline calibration apparatus, constructed to be a near-identical version of the main vacuum chamber, except with improved optical access for a temperature probe laser. The probe laser is coherently split between two arms of a Michelson interferometer (Fig. 3). The resulting fringe shifts are proportional to changes in substrate temperature. To test the robustness of the calibration and the uniformity of the substrate temperature, the calibration was repeated several times as the details of the alignment of the probe lasers and of the heating laser were varied. A finite-element numerical model of the thermal system agreed with our measurements and contributed to our confidence that the temperature of the substrate and the environment were understood. Residual systematic uncertainties in temperature are reflected in the error bars in Fig. 4(b).

The experiment, described in detail in [9], begins with an adiabatic displacement of the atom cloud to a distance  $x$  from the bottom surface ( $+\hat{x}$  face) of the substrate via the addition of a vertical bias magnetic field. The cloud is then resonantly driven into a mechanical dipole oscillation by an oscillatory magnetic field [29]. After a period of free oscillation the relative position of the cloud is determined by transferring the atoms to the anti-trapped  $|F = 2, m_F = -2\rangle$  state via an adiabatic rapid passage. The atoms fall rapidly away from the minimum of the magnetic-trapping field and are destructively imaged on the  $|F = 2, m_F = -2\rangle \rightarrow |F' = 3, m_{F'} = -3\rangle$  cycling transition.

This process is repeated for various times in the free oscillation. The center-of-mass position is recorded at short times to determine the initial phase of the oscillation and at later times ( $\sim 1$ s) to precisely determine the oscillation frequency. Data is taken consecutively alternating the trap center position between a distance  $x$ , close to the surface, and a normalizing distance  $x_o = 15 \mu\text{m}$ . The distance  $x_o$  is sufficiently far from the substrate to

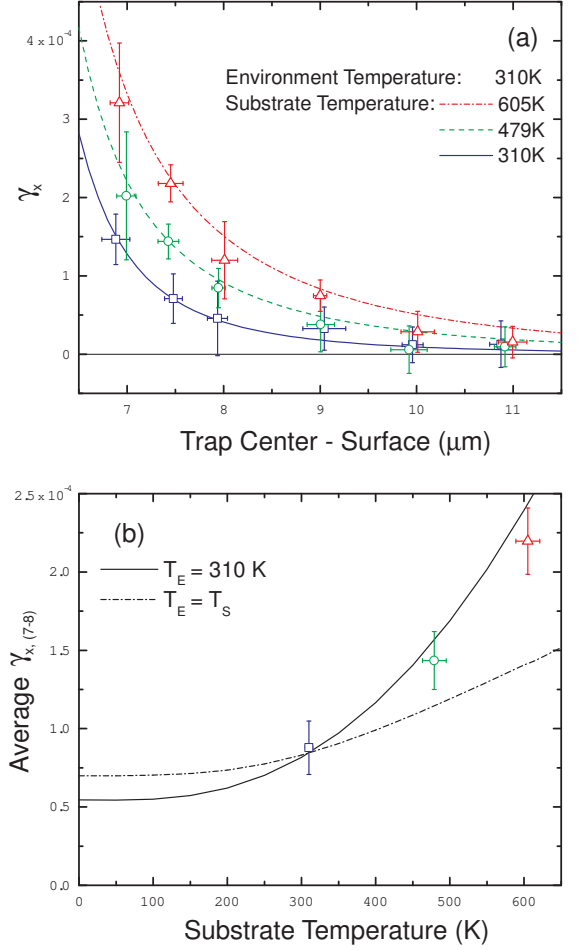


FIG. 4: (Color online) (a) Fractional change in the trap frequency due to the Casimir-Polder force. Pictured are three sets of data and accompanying theoretical curves for various substrate temperatures. The blue squares represent data taken with a 310 K substrate; green circles, a 479 K substrate; and red triangles, a 605 K substrate. The environment temperature is maintained at 310 K. The error bars represent the total uncertainty (statistical and systematic) of the measurement. (b) Average values of  $\gamma_x$  from (a) (for trap center to surface positions 7.0, 7.5, and 8.0  $\mu\text{m}$ ) plotted versus substrate temperature. These values further demonstrate the clear increase in strength of the C-P force for elevated temperatures. The solid theory curve represents the nonequilibrium effect (corresponding 7–8  $\mu\text{m}$  average) in which substrate and environment are at unequal temperatures, while the dash-dot theory curve represents the case of equal temperatures.

avoid surface perturbations, yet close enough to provide a local oscillator  $\omega_o$  with which the data taken at  $x$  can be compared. Data sets are then taken at a number of surface-atom positions (between 7–11  $\mu\text{m}$ ) and for various substrate temperatures (between 310 and 605 K).

The results in Fig. 4(a) show the fractional change in the trap frequency  $\gamma_x$  plotted as a function of the trap center to surface position  $x$ . The blue squares show the measured effect of the room-temperature Casimir-

Polder force ( $T_S=310(5)$  K) on the trap frequency. The increase in the strength of the C-P force due to thermal corrections becomes obvious when the substrate is heated to 479(16) K (green circles) and even more pronounced when it is at 605(16) K (red triangles). These measurements were all done maintaining a room temperature environment for which the pyrex vacuum chamber walls were measured to be  $T_E = 310(5)$  K. The curves in Fig. 4(a) represent the theoretical predictions [24] for corresponding substrate-environment temperature scenarios, showing excellent agreement with the measurements. Each data point pictured represents the average of three or four data sets taken at a given distance and temperature, while the error bars represent the total error in the measurement (systematic and statistical).

For statistical clarity in data analysis, the average value of  $\gamma_x$  can be computed for each substrate temperature (using trap center to surface positions 7.0, 7.5, and 8.0  $\mu\text{m}$  only). These values, plotted in Fig. 4(b), clearly show a significant increase in the strength of the Casimir-Polder force for hotter substrate temperatures; they also distinguish the nonequilibrium theory curve (solid) from the equilibrium (dash-dot), for which a much smaller force increase is predicted.

Techniques described in previous work [9] demonstrate the ability to differentiate the Casimir-Polder force from spurious forces caused by electric and magnetic fields from surface contaminants. These techniques were also employed in this work for all three scenarios in Fig. 4(a), none of which showed significant surface contamination. We can rule out that the measured increase in strength of the C-P force comes from any of the following: an increase in the dielectric constant with increasing temperature, mechanical effects on the atoms from the heating laser, thermal radiation from the substrate reflecting from the vacuum chamber walls, or environment radiation penetrating through the substrate from above. One also must consider the quality of the blackbody radiation emitted by the environment. While the pyrex walls of the chamber are transparent at visible and near-infrared wavelengths, at 5–10  $\mu\text{m}$  wavelengths the walls are opaque, with an emissivity  $> 0.8$ . The relatively large surface area of the chamber walls, compared to that of the substrate, also helps ensure that the environmental radiation approaches the ideal 310 K spectrum.

In conclusion, we have made the first measurement discerning the temperature dependence of the Casimir-Polder force and confirmed the nonequilibrium theory of Antezza *et al.* [24]. The strength of this force was shown to increase by a factor of nearly three as the substrate temperature doubles.

We are grateful for experimental assistance from C. Gillespie and useful discussions with C. Henkel, G. Roati, D. Harber, and the JILA BEC collaboration. This work was supported by grants from the NSF and NIST and is based upon work supported under a NSF

Graduate Research Fellowship.

- 
- [\*] electronic address: john.obrecht@colorado.edu
  - [†] Quantum Physics Division, National Institute of Standards and Technology.
  - [1] T. Ederth, Phys. Rev. A **62**, 062104 (2000).
  - [2] J. Chiaverini, S. J. Smullin, A. A. Geraci, D. M. Weld and A. Kapitulnik, Phys. Rev. Lett. **90**, 151101 (2003).
  - [3] R. S. Decca, D. Lopez, E. Fischbach, G. L. Klimchitskaya, D. E. Krause, V. M. Mostepanenko, Ann. Phys. (N.Y.) **318**, 37 (2005).
  - [4] S. K. Lamoreaux, Phys. Rev. Lett. **78**, 5 (1997).
  - [5] H. B. G. Casimir, Proc. K. Ned. Akad. Wet. **51**, 793 (1948).
  - [6] H. B. G. Casimir and D. Polder, Phys. Rev. **73**, 360 (1948).
  - [7] M. Antezza, L. P. Pitaevskii, S. Stringari, and V. B. Svetovoy, cond-mat/0607205 (2006).
  - [8] J. M. McGuirk, D. M. Harber, J. M. Obrecht, and E. A. Cornell, Phys. Rev. A **69**, 062905 (2004).
  - [9] D. M. Harber, J. M. Obrecht, J. M. McGuirk, and E. A. Cornell, Phys. Rev. A **72**, 033610 (2005).
  - [10] E. M. Lifshitz, Doklady Akademii Nauk SSSR **100**, 879 (1955).
  - [11] S. K. Lamoreaux, Rep. Prog. Phys. **68**, 201 (2005).
  - [12] P. H. G. M. van Blokland and J. T. G. Overbeek, J. Chem. Soc. Faraday Trans. I **74**, 2637 (1978).
  - [13] U. Mohideen and A. Roy, Phys. Rev. Lett. **81**, 4549 (1998).
  - [14] H. B. Chan, V. A. Aksyuk, R. N. Kleiman, D. J. Bishop, and F. Capasso, Science **291**, 1941 (2001).
  - [15] G. Bressi, G. Carugno, R. Onofrio, and G. Ruoso, Phys. Rev. Lett. **88**, 041804 (2002).
  - [16] R. S. Decca, D. Lopez, E. Fischbach, and D. E. Krause, Phys. Rev. Lett. **91**, 050402 (2003).
  - [17] C. I. Suenik, M. G. Boshier, D. Cho, V. Sandoghdar, and E. A. Hinds, Phys. Rev. Lett. **70**, 560 (1993).
  - [18] A. Landragin, J. Y. Courtois, G. Labeyrie, N. Vansteenkiste, C. I. Westbrook, and A. Aspect, Phys. Rev. Lett. **77**, 1464 (1996).
  - [19] F. Shimizu, Phys. Rev. Lett. **86**, 987 (2001).
  - [20] V. Druzhinina and M. DeKieviet, Phys. Rev. Lett. **91**, 193202 (2003).
  - [21] Y. J. Lin, I. Teper, C. Chin, and V. Vuletic, Phys. Rev. Lett. **92**, 050404 (2004).
  - [22] T. A. Pasquini, Y. Shin, C. Sanner, M. Saba, A. Schirotzek, D. E. Pritchard, and W. Ketterle, Phys. Rev. Lett. **93**, 223201 (2004).
  - [23] H. Oberst, Y. Tashiro, K. Shimizu, and F. Shimizu, Phys. Rev. A **71**, 052901 (2005).
  - [24] M. Antezza, L. P. Pitaevskii, and S. Stringari, Phys. Rev. Lett. **95**, 113202 (2005).
  - [25] This contribution was first considered by C. Henkel, K. Joulain, J.-P. Mulet, and J.-J. Greffet, J. Opt. A: Pure Appl. Opt. **4**, S109 (2002).
  - [26] Here we assume that the atom does not absorb radiation ( $T_E$  and  $T_S$  are small with respect to atomic resonances).
  - [27] M. Antezza, L. P. Pitaevskii, and S. Stringari, Phys. Rev. A **70**, 053619 (2004).
  - [28] D. M. Harber, J. M. McGuirk, J. M. Obrecht, and E. A.

Cornell, J. Low Temp. Phys. **133**, 229 (2003).

[29] The amplitude of the oscillation is carefully calibrated to be  $2.50(2) \mu\text{m}$  in the  $\hat{x}$  direction for all measurements.